

# Equilibrium spin pulsars unite neutron star populations

Wynn C. G. Ho,<sup>1,2\*</sup> H. Klus,<sup>1,3</sup> M. J. Coe<sup>1,3</sup> and Nils Andersson<sup>1,2</sup>

<sup>1</sup>*STAG Research Centre, University of Southampton, Southampton, SO17 1BJ*

<sup>2</sup>*Mathematical Sciences, University of Southampton, Southampton, SO17 1BJ*

<sup>3</sup>*Physics & Astronomy, University of Southampton, Southampton, SO17 1BJ*

Accepted 2013 November 5. Received 2013 November 5; in original form 2013 September 19

## ABSTRACT

Many pulsars are formed with a binary companion from which they can accrete matter. Torque exerted by accreting matter can cause the pulsar spin to increase or decrease, and over long times, an equilibrium spin rate is achieved. Application of accretion theory to these systems provides a probe of the pulsar magnetic field. We compare the large number of recent torque measurements of accreting pulsars with a high-mass companion to the standard model for how accretion affects the pulsar spin period. We find that many long spin period ( $P \gtrsim 100$  s) pulsars must possess either extremely weak ( $B < 10^{10}$  G) or extremely strong ( $B > 10^{14}$  G) magnetic fields. We argue that the strong-field solution is more compelling, in which case these pulsars are near spin equilibrium. Our results provide evidence for a fundamental link between pulsars with the slowest spin periods and strong magnetic fields around high-mass companions and pulsars with the fastest spin periods and weak fields around low-mass companions. The strong magnetic fields also connect our pulsars to magnetars and strong-field isolated radio/X-ray pulsars. The strong field and old age of our sources suggests their magnetic field penetrates into the superconducting core of the neutron star.

**Key words:** accretion, accretion discs – pulsars: general – stars: magnetars – stars: magnetic field – stars: neutron – X-rays: binaries

## 1 INTRODUCTION

The vast majority of the more than 2000 known neutron stars are observed in the radio as rotation-powered pulsars, which lose rotational energy and spin down due to their electromagnetic radiation. Measurement of the rate of energy loss, or spin-down rate, allows one to infer the pulsar magnetic field  $B$  (Gunn & Ostriker 1969; Spitkovsky 2006). However the spin-down torque due to electromagnetic radiation ( $\sim -10^{30}$  erg  $B_{12}^2 P^{-3}$ , where  $B_{12} = B/10^{12}$  G and  $P$  is the spin period) is relatively weak compared to torque due to matter accretion by the neutron star from a close binary companion. In this latter case, interactions between the pulsar magnetic field and matter from the companion star produces a torque ( $\sim \pm 10^{34}$  erg  $\dot{M}_{-9}^{6/7} B_{12}^{2/7}$ , where  $\dot{M}_{-9} = \dot{M}/10^{-9} M_{\odot} \text{ yr}^{-1}$  and  $\dot{M}$  is the mass accretion rate) which can spin the pulsar up or down, depending on whether matter is accreted or ejected. By measuring the rate of change in spin period  $\dot{P}$  (which is related to torque  $N$  by  $N = -2\pi I \dot{P}/P^2$ , where  $I$  is the stellar moment of inertia), one can obtain insights into the physics that governs the accretion process, including important properties such as

the role of the magnetic field. However, observing the long-term  $\dot{P}$  in accretion-powered pulsars is very difficult due to short-term fluctuations, with approximately twenty sources detected (see Klus et al. 2013a, and references therein).

Our study is based on the work of Klus et al. (2013b), who report a detailed analysis of Rossi X-ray Timing Explorer (RXTE) observations of high-mass X-ray binaries (HMXBs) in the Small Magellanic Cloud, specifically pulsar systems with an OBe main sequence companion; these sources are designated Small Magellanic Cloud X-ray pulsars (SXPs) (Coe et al. 2005). The data set spans 13 years and contains 42 sources for which the spin period  $P$  and count rate as a function of time have been measured. Spin period time derivatives  $\dot{P}$  are calculated from the former, and X-ray luminosities  $L$  are determined from the latter and can be related to mass accretion rate by  $\dot{M} = LR/GM$ , where  $M$  and  $R$  are the neutron star mass and radius, respectively. From their binary parameters, Klus et al. (2013b) find that matter accretes onto the neutron star in each SXP system via an accretion disk (c.f. wind). Different methods are then used to determine the magnetic field of each pulsar.

Here we extend the work of Klus et al. (2013b). In Section 2, we examine torque models, especially that of the standard disk accretion model of Ghosh & Lamb (1979b) and Kluźniak & Rappaport (2007), and demonstrate a simple

\* Email: wynnho@slac.stanford.edu

method for matching the detailed result of Ghosh & Lamb (1979b). In Section 3, we show that the standard model can explain fast-spinning, weak magnetic field pulsars in low-mass X-ray binaries (LMXBs) and slow-spinning, strong field pulsars in HMXBs, and we consider the broader context of neutron star magnetic fields in light of our findings. We summarize in Section 4.

## 2 STANDARD DISK ACCRETION MODEL AND EQUILIBRIUM SPIN PULSARS

Figure 1 shows the spin period time derivative  $\dot{P}$  as a function of spin period  $P$  for known pulsars. For isolated sources, i.e., those not in a binary system, pulsars with the highest  $\dot{P}$  values are magnetars, i.e., neutron stars that predominantly have magnetic fields  $B \gtrsim 10^{14}$  G and can exhibit a variety of high-energy emission (Woods & Thompson 2006; Mereghetti 2008). The vast majority of sources are normal rotation-powered radio pulsars whose spin-down rate (i.e.,  $\dot{P} > 0$ ) is measured very accurately from coherent timing analysis (Lyne & Graham-Smith 1998). The pulsar magnetic field is then estimated by assuming that the electromagnetic energy radiated produces a torque (after using the conversion: torque =  $-2\pi I\dot{P}/P^2$ )

$$\dot{P} \approx 9.8 \times 10^{-16} \text{ s s}^{-1} R_6^6 I_{45}^{-1} B_{12}^2 P^{-1}, \quad (1)$$

where  $R_6 = R/10$  km and  $I_{45} = I/10^{45}$  g cm<sup>2</sup>. While the exact nature of the mechanism that causes radio emission is not known for certain, there is general agreement that there exists a “death line” below which observable emission ceases (Ruderman & Sutherland 1975; Bhattacharya et al. 1992). An example death line is shown in Fig. 1.

In contrast to radio pulsars, the period derivative of accreting neutron stars in an X-ray binary is determined by measuring and finding the difference between the spin period at different epochs (see, e.g., Townsend et al. 2011). We see from Fig. 1 that  $\dot{P}$  for accreting pulsars with  $P \gtrsim 1$  s, such as the SXPs, is much larger than that of most radio pulsars and that  $\dot{P}$  for SXPs is comparable to other previously-known long spin period sources. All these pulsars possess a binary companion (some companions are low-mass stars and others are high-mass main sequence or supergiant stars) from which the neutron stars are accreting. Because accretion is thought to suppress radio emission (Bhattacharya & van den Heuvel 1991; Archibald et al. 2009) and the torque from accretion is much stronger than that of electromagnetic spin-down (see Sec. 1), the magnetic field of accreting pulsars in a LMXB or HMXB cannot be estimated using eq. (1). To determine their magnetic field, one can use the standard disk accretion model of Ghosh & Lamb (1979b) (see also Ghosh & Lamb 1979a; we also examine the model of Kluźniak & Rappaport 2007, see below). This model is based on detailed calculations of the interaction between a rotating pulsar magnetosphere and an accretion disk surrounding the pulsar. The predicted torque yields

$$\dot{P} = -4.3 \times 10^{-5} \text{ s yr}^{-1} M_{1.4}^{-3/7} R_6^{6/7} I_{45}^{-1} \times n(\omega_s) \mu_{30}^{2/7} \left( PL_{37}^{3/7} \right)^2, \quad (2)$$

where  $M_{1.4} = M/1.4 M_\odot$ ,  $\mu_{30} = \mu/10^{30}$  G cm<sup>3</sup>,  $\mu (= BR^3)$  is the magnetic moment of the neutron star, and  $L_{37} = L/10^{37}$  erg s<sup>-1</sup>, and is shown in Fig. 2 for three values of

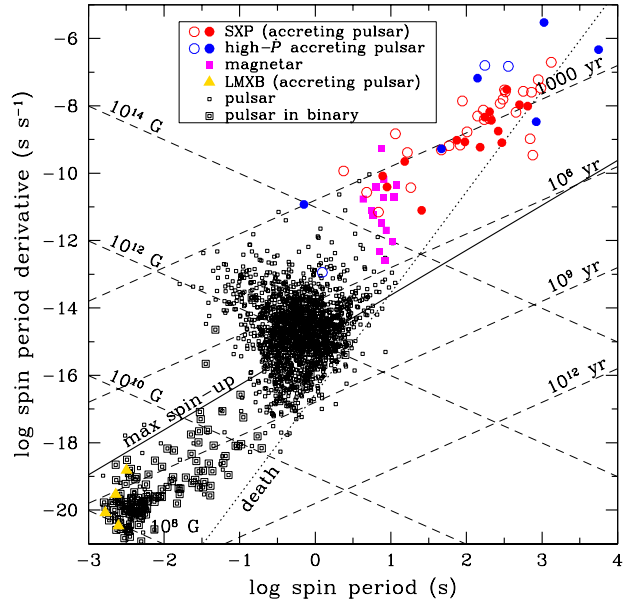


**Figure 1.** Pulsar spin period  $P$  versus spin period time derivative  $\dot{P}$ . Open squares are pulsar values taken from the ATNF Pulsar Catalogue (Manchester et al. 2005), and solid squares denote magnetars. Open and closed circles denote (accreting) sources that have  $\dot{P} < 0$  and  $\dot{P} > 0$ , respectively (Klus et al. 2013a, and references therein; Esposito et al. 2013; Klus et al. 2013b). Triangles denote (accreting) LMXBs (Patruno 2010; Haskell & Patruno 2011; Riggio et al. 2011). The dashed lines indicate spin-down age ( $= P/2\dot{P}$ ) and inferred magnetic field [ $= 3.2 \times 10^{19}$  G  $(P\dot{P})^{1/2}$ ]. The dotted line indicates the (theoretically uncertain) death line for pulsar radio emission; note that the death line shown here is calculated using eq. (1) and therefore does not apply to accreting pulsars (c.f. Fig. 4). The solid line indicates the minimum  $P$  and maximum  $\dot{P}$  that a pulsar can possess as a result of matter accretion from a binary companion.

the magnetic field. Hereafter we ignore mass and radius dependencies since they can only vary by a factor of about two while the magnetic field can vary by several orders of magnitude. The dimensionless torque  $n(\omega_s)$  accounts for coupling between the magnetic field and the disk plasma (Ghosh & Lamb 1979b) (see also Wang 1995) and depends on the fastness parameter  $\omega_s [= \Omega/\Omega_K(r_m)]$ , which is given by

$$\omega_s = 3.3 \xi^{3/2} M_{1.4}^{-2/7} R_6^{-3/7} \mu_{30}^{6/7} \left( PL_{37}^{3/7} \right)^{-1}. \quad (3)$$

$\Omega = 2\pi/P$  is the pulsar spin frequency,  $\Omega_K(r_m)$  is the Kepler orbital frequency at radius  $r_m [= \xi r_A = \xi(GM\mu^4/2R^2L^2)^{1/7}]$ , where the energy density of accreting matter transitions from being kinetically to magnetically dominated, and  $\xi \approx 1$  (see, e.g., Wang 1996). The sign of the dimensionless torque  $n(\omega_s)$  is determined by whether the centrifugal force due to stellar rotation ejects matter and spins down the star (“fast rotator” regime with  $\omega_s > 1$ ) or accretes matter and spins up the star (“slow rotator” regime with  $\omega_s < 1$ ) (see, e.g., Wang 1995). It is important to note that a long spin period ( $P \gg 1$  s) pulsar can still be classified as a fast rotator since the fastness parameter  $\omega_s$  depends on the strength of the pulsar magnetic field.

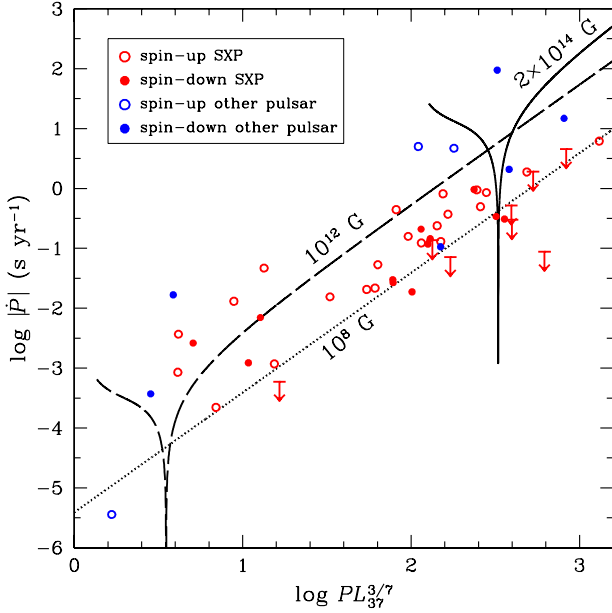


**Figure 2.** Rate of change of spin period  $\dot{P}$  versus  $PL^{3/7}$ . Open and closed circles denote sources that have  $\dot{P} < 0$  and  $\dot{P} > 0$ , respectively (Klus et al. 2013a, and references therein; Esposito et al. 2013; Klus et al. 2013b). The lines indicate the theoretical prediction from the standard disk accretion model of Ghosh & Lamb (1979b) with different values of magnetic field [see eq. (2)].

A good approximation to eq. (2) can be derived very simply. Matter accreting at the magnetosphere transition  $r_m$  has specific angular momentum

$$l_{\text{acc}} = \pm r_m^2 \Omega_K, \quad (4)$$

while matter rotating with the magnetosphere at  $r_m$  has specific angular momentum

$$l_m = r_m^2 \Omega. \quad (5)$$

Assuming prograde rotation between the accretion disk and neutron star (i.e.,  $l_{\text{acc}} > 0$ ), the total torque on the neutron star is then

$$N_{\text{tot}} = N_{\text{acc}} + N_m = \dot{M} \Delta l = \dot{M} r_m^2 \Omega_K (1 - \omega_s), \quad (6)$$

which gives

$$\begin{aligned} \dot{P} &= -7.1 \times 10^{-5} \text{ s yr}^{-1} \xi^{1/2} M_{1.4}^{-3/7} R_6^{6/7} I_{45}^{-1} \\ &\times (1 - \omega_s) \mu_{30}^{2/7} (PL_{37}^{3/7})^2. \end{aligned} \quad (7)$$

Figure 3 shows that eq. (7) agrees with eq. (2) to within  $\approx 15\%$  over a large range in  $PL^{3/7}$ , except when  $\omega_s$  approaches and exceeds unity. Similar accuracy is obtained as the magnetic field is varied over many orders of magnitude.

The linear dependence of  $\log \dot{P}$  at relatively high values of  $\log PL^{3/7}$  is simply the result of the standard *spin-up* torque  $\dot{M}(GM_{r_m})^{1/2}$  due to disk accretion (for prograde rotation, or spin-down torque for retrograde rotation) and is the first term  $N_{\text{acc}}$  in eq. (6) (Pringle & Rees 1972; Rappaport & Joss 1977). In the slow rotator regime [ $\omega_s \ll 1$ ; see eq. (3)], the rate of change of spin period  $\dot{P}$  is simply given by  $N_{\text{acc}}$ , and the magnetic field is  $B \propto \dot{P}^{7/2}$ .

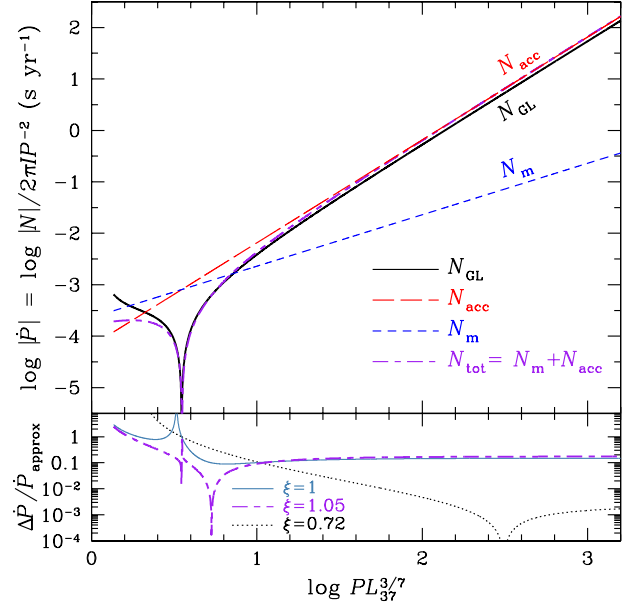


**Figure 3.** Top panel: Rate of change of spin period  $\dot{P}$  versus  $PL^{3/7}$  for  $B = 10^{12}$  G. The solid line labeled  $N_{\text{GL}}$  indicates the theoretical prediction of Ghosh & Lamb (1979b) [see eq. (2)]. The short-long-dashed line labeled  $N_{\text{tot}}$  indicates the analytic approximation given by eq. (7). Bottom panel: Relative difference between the exact and approximate values of  $\dot{P}$  for different values of  $\xi$  [see eq. (3)].

The second term in eq. (6) is the *spin-down* torque due to mass accretion onto a rotating object. These two torques and their total (recall that  $N = -2\pi I \dot{P}/P^2$ ) are shown in Fig. 3. We note that an equation similar to eq. (6) is given in Shakura et al. (2012) but with different coefficients for  $N_{\text{acc}}$  and  $N_m$ .

The sharp decrease and then increase in  $\dot{P}$  for  $B = 10^{12}$  G (and  $2 \times 10^{14}$  G in Fig. 2) is due to the change of sign from  $\dot{P} < 0$  (spin-up) to  $\dot{P} > 0$  (spin-down). This marks the fast rotator regime near spin equilibrium ( $\omega_s \approx 1$ ) (Davidson & Ostriker 1973; Alpar et al. 1982; Wang 1987; Kluźniak & Rappaport 2007): After sustained epochs of spin-up and spin-down, a steady state will be achieved where the net torque on the pulsar is negligible ( $\dot{P} \sim 0$ ). The resulting equilibrium spin pulsar (ESP) spins near the period

$$P_{\text{eq}} = 23 \text{ s } \xi^{3/2} M_{1.4}^{-2/7} R_6^{15/7} L_{37}^{-3/7} (B/10^{13} \text{ G})^{6/7}, \quad (8)$$

which is obtained by setting  $\omega_s = 1$  in eq. (3). Note that for spin equilibrium at  $\omega_s \sim 0.35$  (Ghosh & Lamb 1979b), the coefficient in eq. (8) becomes 67 s, and the inferred magnetic field is lower by a factor of  $(0.35)^{7/6} \sim 0.3$ .

### 3 COMPARISON TO SXP OBSERVATIONS

Previously only  $\sim 20$  X-ray pulsars have had large torques (i.e.,  $\dot{P}$ ) measured (see, e.g., Klus et al. 2013a). Figure 2 shows these, as well as the 42 SXPs from Klus et al. (2013b). Using the observed values of  $P$ ,  $\dot{P}$ , and  $L$  for each SXP, Klus et al. (2013b) find that the standard disk accretion model prediction for  $\dot{P}$  with magnetic fields in the range

$B \approx 10^6 - 10^{15}$  G can fit all SXP (the model of Kluźniak & Rappaport yields magnetic fields  $\sim 10 - 20\%$  weaker). In particular, fits to each SXP can yield two possible solutions, either a weak field ( $< 10^{10}$  G) or strong field ( $> 10^{12}$  G). The weak field solution arises from the match between the observed  $\dot{P}$  and the torque  $N_{\text{acc}}$  [c.f.  $N_{\text{tot}}$ ; see eq. (6)] if the pulsar is in the slow rotator regime (see also Fig. 3). On the other hand, if the SXP is in the fast rotator regime near spin equilibrium, then the strong pulsar field is simply determined from eq. (8), and the observed  $\dot{P}$  is due to small fluctuations around torque balance ( $N_{\text{acc}} \approx N_{\text{m}}$ ). Both solutions are remarkable and unexpected, based on previous observations of other types of pulsars (see Fig. 4). In the following, we argue for the strong magnetic field solution. We note that, prior to the present work, only four pulsars have been found to possibly be near spin equilibrium (Patruno 2010; Haskell & Patruno 2011; Riggio et al. 2011), although many pulsars in LMXBs are assumed to be in this regime (White & Zhang 1997; Patruno et al. 2012). The strong field solution we find (see also Klus et al. 2013b) suggests that a vast majority of the 42 SXPs are near spin equilibrium and thus are ESPs.

### 3.1 Magnetic Fields: Weak or Strong?

For many SXPs, we find that their observed  $P$ ,  $\dot{P}$ , and  $L$  can be fit with the standard accretion model [eq. (2)] and one of two possible magnetic fields: a relatively weak field ( $< 10^{10}$  G) or strong field ( $> 10^{12}$  G). While either solution is valid, the strong field is more likely from primarily age/timescale arguments. Most neutron stars are born with  $B > 10^{12}$  G, which can be inferred from the lines of magnetic field and spin-down age shown in Fig. 1, as well as from population synthesis studies (Faucher-Giguère & Kaspi 2006; Popov et al. 2010). Therefore if SXPs have weak magnetic fields, their initial field either decayed to the current level or has been buried below the surface. The global magnetic field in neutron stars decays rather slowly and on the timescale  $\sim 10^6$  yr (Haensel et al. 1990; Goldreich & Reisenegger 1992; Glampedakis et al. 2011), while the maximum age of an OBe star is  $\sim 10^7$  yr. Thus there is insufficient time for the field to decay the many orders of magnitude required. Burial of the field by accretion (Romani 1990) is unlikely in so many SXPs because of the very short time over which a large amount of accretion must take place (Chevalier 1989; Geppert et al. 1999). On the other hand, if SXPs have strong magnetic fields, then many are currently near spin equilibrium, which they can easily achieve given their short spin-evolution timescale ( $P/|\dot{P}| \sim 10^3$  yr) compared to their age. Finally, spin equilibrium also allows spin-down ( $\dot{P} > 0$ ) without retrograde rotation.

### 3.2 Connection to LMXBs and millisecond pulsars

The evolutionary scenario that leads to the formation of fast-spinning ( $P \lesssim 10$  ms, hence millisecond) pulsars is briefly described here (see, e.g., Alpar et al. 1982; Bhattacharya & van den Heuvel 1991; Tauris 2012). A millisecond pulsar begins as a standard pulsar in a wide binary that has spun down past the death line. This pulsar can be brought back to radio activity by accreting matter from its

(low-mass) companion star, either when the orbit shrinks due to gravitational radiation or the companion evolves off the main sequence. Accretion of matter spins up the pulsar, thus recycling it back from beyond death, although it is only seen as a millisecond radio pulsar after accretion ceases. However some pulsars are observed in the X-rays which are emitted during the accretion process, and these are the LMXBs (Bildsten et al. 1997). Thus LMXBs are predecessors of millisecond radio pulsars. In this scenario, there is a lower limit to the spin period that accretion can produce. This minimum period is obtained by considering a pulsar that has reached spin equilibrium through accretion at the maximum accretion rate or luminosity  $\sim 10^{38}$  erg s $^{-1}$ , above which radiation pressure prevents further accretion. Equation (8) then yields the magnetic field of the pulsar, and these fields turn out to be low for LMXBs ( $B \sim 10^8 - 10^9$  G). After accretion ceases, the pulsar spins down by the standard electromagnetic energy loss. The resulting maximum spin-up line is shown in Fig. 1. We see that almost all observed pulsars which are likely to be recycled are below this line and above the death line.

Figure 4 shows the magnetic field and spin period of known pulsars. The magnetic field of rotation-powered pulsars are obtained from their  $P$  and  $\dot{P}$  and using eq. (1). Only four LMXBs have a measured  $\dot{P}$  or upper limit on  $\dot{P}$ , and spin equilibrium is assumed in order to calculate their magnetic field. Many LMXBs have large distance errors which affects the determination of their luminosity. Thus their inferred magnetic fields are very uncertain, and this uncertainty limits our ability to understand the physics of accretion using LMXBs.

The SXPs bridge this gap in knowledge. The weak magnetic field solution to these pulsars would place them in the extreme bottom right of Fig. 4, in a region far away from all previously known sources, and thus is not shown. Instead we show the strong magnetic field solution, which is determined from their measured spin period and X-ray luminosity and eq. (8) since SXPs are near spin equilibrium for this solution. The shaded region in Fig. 4 is the spin equilibrium region for the range of luminosities [ $L = (0.2 - 4) \times 10^{37}$  erg s $^{-1}$ ] spanned by our sources. Evidently SXPs (as ESPs) are governed by the same accretion physics as that used to explain the recycling of LMXBs into millisecond pulsars even though the physics regime spans many orders of magnitude in magnetic field. While LMXBs, with their low magnetic fields ( $B \sim 10^8 - 10^9$  G), produce pulsars with millisecond spin periods, SXPs, with their high magnetic fields ( $B \sim 10^{12} - 10^{15}$  G), produce pulsars with long spin periods ( $P \gtrsim 10$  s). An important difference between the LMXBs and SXPs is that the latter are now known to be close to spin equilibrium, as well as having a more accurate distance, and thus their magnetic fields are much better determined.

### 3.3 Connection to magnetars and high- $B$ pulsars

The strong magnetic field of SXPs spans a wide range ( $B \approx 10^{12} - 10^{15}$  G), similar to the range for rotation-powered pulsars. There are also  $< 20$  Galactic HMXBs for which electron cyclotron spectral lines have been detected; however there is uncertainty in where these lines are generated and likely selection effects (see Klus et al. 2013b, for more details). Of particular note are those 24 of 42 SXPs



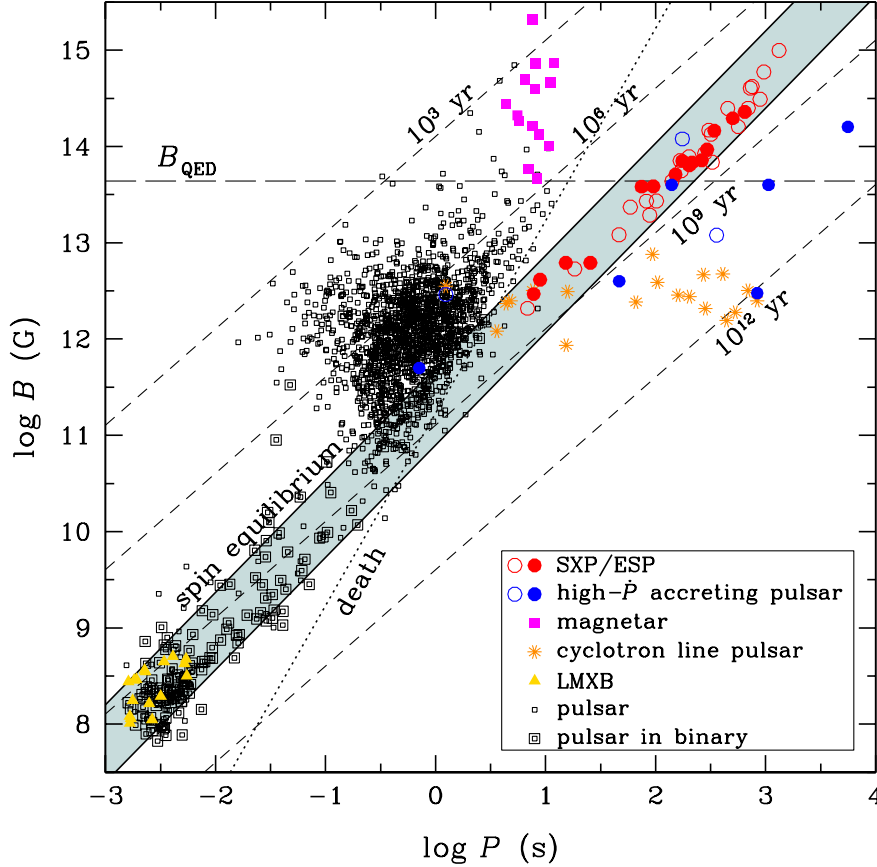


**Figure 4.** Pulsar magnetic field  $B$  versus spin period  $P$ . Open squares are pulsars from the ATNF Pulsar Catalogue (Manchester et al. 2005), and solid squares denote magnetars. Open and closed circles denote sources that have  $\dot{P} < 0$  and  $\dot{P} > 0$ , respectively (Ghosh & Lamb 1979b; Baykal et al. 2002; Cui & Smith 2004; Ikhshanov 2012; Reig et al. 2012; Klus et al. 2013a,b). Triangles denote LMXBs (Patruno et al. 2012). Stars denote high mass X-ray binaries whose field is determined from an electron cyclotron spectral line (see <http://www.sternwarte.uni-erlangen.de/wiki/doku.php?id=cyclo:start>). The short-dashed lines indicate spin-down age ( $= P/2\dot{P}$ ), the long-dashed line indicates the QED field  $B_{\text{QED}} = 4.414 \times 10^{13}$  G, and the dotted line indicates the (theoretically uncertain) death line for pulsar radio emission. The solid lines bounding the shaded region indicate the  $B$  and  $P$  [see eq. (8)] that a pulsar can possess as a result of accretion from a binary companion at the mass accretion rate observed for SXP/ESPs (red circles).

with  $B > B_{\text{QED}} = m_e^2 c^3 / e \hbar = 4.414 \times 10^{13}$  G, where  $B_{\text{QED}}$  is the critical quantum electrodynamics (QED) magnetic field (and 13 SXPs have  $B > 10^{14}$  G). There are about two dozen previously known neutron stars ( $\sim 1\%$  of the total population) with these fields. They are composed of magnetars, which are strong X-ray/gamma-ray sources and can undergo transient outbursts both of which are powered by their strong magnetic fields (Woods & Thompson 2006; Mereghetti 2008), and high- $B$  pulsars, which behave similar to the bulk of the radio pulsars (Ng & Kaspi 2011). The difference between these two groups could be due to the strength of internal toroidal fields (Pons & Perna 2011). Magnetar-like behavior has not been seen in SXPs, which indicates SXPs with  $B > B_{\text{QED}}$  are in the latter group and possess weak toroidal fields. This may suggest that formation of high- $B$  pulsars is more efficient than that of magnetars and there exists many more of the former than latter.

The relative number of SXPs with superstrong fields ( $B > B_{\text{QED}}$ ) is much higher than in the normal pulsar population. On the one hand, this significantly higher

fraction of highly-magnetized neutron stars could be due to inherently different source populations, e.g., neutron star formation as a result of an electron capture supernova (Nomoto 1984; Podsiadlowski et al. 2004) or accretion induced collapse (Nomoto 1984; Taam & van den Heuvel 1986; Nomoto & Kondo 1991). On the other hand, selection effects could be hindering detection of isolated highly-magnetized neutron stars. Effects include X-ray absorption, radio dispersion, and/or quenching of radio emission beyond the death line, and some of these effects are taken into account in population synthesis models (see, e.g., Faucher-Giguère & Kaspi 2006; Popov et al. 2010). Note that for SXPs, their rotational energy loss rate  $\dot{E}$  [ $= 4\pi^2 I \dot{P} / P^3$  and using eq. (1)] is  $\sim 4 \times 10^{25} \text{ erg s}^{-1} (B/10^{13} \text{ G})^2 (P/100 \text{ s})^{-4}$ . In addition, magnetars and high- $B$  pulsars have a short spin-down timescale ( $\approx 10^3 - 10^5$  yr; see Figs. 1 and 4) and are young (age on the same order as their spin-down timescale). Meanwhile, the high-mass companion of SXPs has a much longer lifetime ( $\sim$  a few  $\times 10^6$  yr), which allows us to study the pulsars at

later stages in their life. In other words, it is only because of accretion that we are able to detect these highly-magnetized neutron stars when they are older than when they are young and isolated (see also Chashkina & Popov 2012). This may suggest that magnetic field decay in neutron stars occurs slower than previously thought (Pons et al. 2009) and could be the result of the magnetic field extending into the superconducting neutron star core, where the field decay timescale is much longer (Glampedakis et al. 2011). Importantly, this scenario where all pulsars are drawn from the same source population would resolve the neutron star birthrate problem (Keane & Kramer 2008; Watters & Romani 2011) and support a unified picture of neutron stars (Keane & Kramer 2008; Kaspi 2010; Popov et al. 2010).

#### 4 SUMMARY

Using recent measurements of a large number of spin period time derivatives  $\dot{P}$  for pulsars in high-mass binaries in the Small Magellanic Cloud (Klus et al. 2013b), we examined the torque implications for the standard disk accretion model (Ghosh & Lamb 1979b) and model of Kluzniak & Rappaport (2007) and for neutron star magnetic fields. We find several interesting results. Many of the 42 SXP are near spin equilibrium, where torques that increase and decrease the spin period are balanced, and thus SXPs are ESPs; previously only four pulsars have been found to possibly be near spin equilibrium. The standard disk accretion model links SXPs (which have high mass companion stars) with pulsars at very short spin periods (which have low mass companions); this is demonstrated by the shaded region in Fig. 4. The strong magnetic field of many SXPs is above the QED-field and links them with magnetars and strong- $B$  radio/X-ray pulsars. The decay of magnetic field in SXPs occurs after  $10^6$  yr, suggesting magnetic field penetration into the superconducting pulsar core. It is possible there are many more superstrong magnetic field pulsars in the Galaxy that remain as yet undetected.

#### ACKNOWLEDGMENTS

We thank the anonymous referee for helpful comments. WCGH and NA acknowledge support from the Science and Technology Facilities Council (STFC) in the United Kingdom. HK acknowledges a STFC studentship.

#### REFERENCES

Alpar, M. A., Cheng, A. F., Ruderman, M. A., Shaham, J., 1982, *Nature*, 300, 728  
 Archibald, A. M. *et al.*, 2009, *Science*, 324, 1411  
 Baykal, A., Stark, M. J., Swank, J. H., 2002, *ApJ*, 569, 903  
 Bhattacharya, D., van den Heuvel, E. P. J., 1991, *Phys. Rep.*, 203, 1  
 Bhattacharya, D., Wijers, R. A. M. J., Hartman, J. W., Verbunt, F., 1992, *A&A*, 254, 198  
 Bildsten, L., *et al.*, 1997, *ApJS*, 113, 367  
 Chashkina, A., Popov S. B., 2012, *New Astron.*, 17, 594  
 Chevalier, R. A., 1989, *ApJ*, 346, 847  
 Coe, M. J., Edge, W. R. T., Galache, J. L., McBride, V. A., 2005, *MNRAS*, 356, 502

Cui, W., Smith, B., 2004, *ApJ*, 602, 320  
 Davidson, K., Ostriker, J. P., 1973, *ApJ*, 179, 585  
 Esposito, P. *et al.*, 2013, *MNRAS*, 433, 2028  
 Faucher-Giguère, C.-A., Kaspi, V. M. 2006, *ApJ*, 643, 332  
 Geppert, U., Page, D., Zannias, T., 1999, *A&A*, 345, 847  
 Ghosh, P., Lamb, F. K., 1979a, *ApJ*, 232, 259  
 Ghosh, P., Lamb, F. K., 1979b, *ApJ*, 234, 296  
 Glampedakis, K., Jones, D. I., Samuelsson, L., 2011, *MNRAS*, 413, 2021  
 Goldreich, P. Reisenegger, A., 1992, *ApJ*, 395, 250  
 Gunn, J. E., Ostriker, J. P. 1969, *Nature*, 221, 454  
 Haensel, P., Urpin, V. A., Yakovlev, D. G., 1990, *A&A*, 229, 133  
 Haskell, B., Patruno, A., 2011, *ApJ*, 738, L14  
 Ikhsanov, N. R., 2012, *MNRAS*, 424, 39  
 Kaspi, V. M., 2010, *Publ. Natl. Acad. Sci.*, 107, 7147  
 Keane, E. F., Kramer, M., 2008, *MNRAS*, 391, 2009  
 Klus, H., Bartlett, E. S., Bird, A. J., Coe, M., Corbet, R. H. D., Udalski, A., 2013a, *MNRAS*, 428, 3607  
 Klus, H., Ho, W. C. G., Coe, M. J., Corbet, R. H. D., Townsend, L. J., 2013b, *MNRAS*, in press  
 Kluzniak, W. & Rappaport, S., 2007, *ApJ*, 671, 1990  
 Lyne, A. G., Graham-Smith, F., 1998, *Pulsar Astronomy*, 2nd ed. Cambridge University Press, Cambridge  
 Manchester, R. N., Hobbs, G. B., Teoh, A., Hobbs, M., 2005, *AJ*, 129, 1993  
 Mereghetti, S., 2008, *A&A Rev.*, 15, 225  
 Ng, C.-Y., Kaspi, V. M., 2011, in Göğüş E., Belloni T., Ertañ Ü., eds, *AIP Conf. Proc. 1379*, *Astrophysics of Neutron Stars 2010*. AIP, Melville, NY, p. 60  
 Nomoto, K., 1984, *ApJ*, 277, 791  
 Nomoto, K., Kondo, Y., 1991, *ApJ*, 367, L19  
 Patruno, A., 2010, *ApJ*, 722, 909  
 Patruno, A, Haskell, B., D'Angelo, C., 2012, *ApJ*, 746, 9  
 Podsiadlowski, Ph., Langer, N., Poelarends, A. J. T., Rappaport, S., Heger, A., Pfahl, E., 2004, *ApJ*, 612, 1044  
 Pons, J. A. & Perna, R., 2011, *ApJ*, 741, 123  
 Pons, J. A., Miralles, J. A., Geppert, U., 2009, *A&A*, 496, 207  
 Popov, S. B., Pons, J. A., Miralles, J. A., Boldin, P. A., Posselt, B., 2010, *MNRAS*, 401, 2675  
 Pringle, J. E., Rees, M. J., 1972, *A&A*, 21, 1  
 Rappaport, S., Joss, P. C., 1977, *Nature*, 266, 683  
 Reig, P., Torrejon, J. M., Blay, P., 2012, *MNRAS*, 425, 595  
 Riggio, A. *et al.*, 2011, *A&A*, 531, A140  
 Romani, R. W., 1990, *Nature*, 347, 741  
 Ruderman, M. A., Sutherland, P. G., 1975, *ApJ*, 196, 51  
 Shakura, N., Postnov, K., Kochetkova, A., Hjalmarsdotter, L., 2012, *MNRAS*, 420, 216  
 Spitkovsky, A., 2006, *ApJ*, 648, L51  
 Taam, R. E., van den Heuvel, E. P. J., 1986, *ApJ*, 305, 235  
 Tauris, T., 2012, *Science*, 335, 561  
 Townsend, L. J., Coe, M. J., Corbet, R. H. D., Hill, A. B., 2011, *MNRAS*, 416, 1556  
 Wang, Y.-M., 1987, *A&A*, 183, 257  
 Wang, Y.-M., 1995, *ApJ*, 449, L153  
 Wang, Y.-M., 1996, *ApJ*, 465, L111  
 Watters, K. P., Romani, R. W., 2011, *ApJ*, 727, 123  
 White, N. E., Zhang, W., 1997, *ApJ*, 490, L87  
 Woods, P. M., Thompson, C., 2006, in Lewin, W. H. G., van der Klis, M., eds, *Compact Stellar X-ray Sources*. Cambridge University Press, Cambridge, p. 547